Analytical Electron Microscopy of Semiconductor Nanowire Functional Materials and Devices for Energy Applications

V P Oleshko[1], E H Williams[1,3], A V Davydov[1], S Krylyuk[1,4], A Motayed[1,4], D Ruzmetov[2,4], T Lam[2], H J Lezec[2] and A A Talin[2,5]

[1]Material Measurement Laboratory and [2]Center for Nanoscale Science and Technology, National Institute of Standards and Technology, Gaithersburg, Maryland 20899, USA
[3]Department of Chemistry and Biochemistry and Department of Electrical and Computer Engineering, George Mason University, Fairfax, Virginia 22030, USA
[4]Institute for Research in Electronics and Applied Physics, University of Maryland, College Park, Maryland 20742, USA
[5]Sandia National Laboratories, Livermore, California 94551, USA

E mail: vladimir.oleshko@nist.gov

Abstract. Functionalized individual semiconductor nanowires (SNWs) and 3D SNW arrays attract a continuously growing interest for applications in optoelectronics, sensing, and energy storage. High-resolution field-emission analytical (scanning) transmission electron microscopy ((S)TEM) enables critical insights into the morphology, crystalline and electronic structures and chemical composition of single-crystalline high-aspect-ratio SNWs as prospective building blocks suitable for both a large scale-up synthesis and fabrication. Furthermore, SNW-based lab-on-a-chip devices may allow direct correlation between functional properties tailored for specific performance and the heterostructure morphology and atomic arrangement of the nanoscale structure being analyzed in various (S)TEM modes.

1. Introduction

High-aspect-ratio semiconductor nanowires (SNWs), often referred to as unconstrained length 1D nanostructures, reveal interesting physical properties that are not seen in bulk semiconductors. SNWs have therefore recently attracted much attention for exploring new physics in reduced dimensions and complex geometries. From a practical point of view, there is a growing interest in the fabrication of SNW-based lab-on-a-chip (opto) electronic devices and chemi-resistive chemical and biological sensors, which have the ability to selectively detect traces of certain chemical compounds or bind biomolecules through resistivity-dependent mechanisms. Functionalized individual Si, SiC and GaN

SNWs and 3D SNW arrays have recently shown potential as (a) a new biosensing platform for selective protein immobilization [1], (b) UV-assisted SNW-MO_2(-Pt) (M=Ti, Sn) hybrid chemical sensors for detection of environmental industrial pollutants and traces of explosives [2,3], and (c) scaffolding templates for renewable energy transducers and storage systems, i.e. miniature all solid-state SNW core – multishell rechargeable Li-ion batteries [4].

Here we report on the characterization of functionalized SNWs and energy related devices by high-resolution field-emission analytical (S)TEM, electron diffraction, and tomography to provide insights into morphology, crystalline and electronic structures, and chemical composition of prospective nano-sized building blocks that are suitable both for a large scale-up synthesis and fabrication using existing semiconductor technologies in a variety of emerging nanotechnology applications.

2. Experimental details

Si NWs were grown in a horizontal hot-wall reactor by chemical vapor deposition (CVD) with metal catalyst particles (Au) utilized to facilitate the vapor-liquid-solid (VLS) growth mechanism [1]. For fabrication of Li-ion nanobatteries (NW-LiBs), as-grown Si NWs were coated with 10 nm of Ti, followed by about 30 nm of Pt, 40 nm of Ti, and a 180 nm-thick layer of $LiCoO_2$. All layers have been deposited using physical vapor deposition in the same chamber without exposure to air. The coated NWs were then annealed in oxygen at 700^o C for 2 hours. Following annealing, the samples were sputter-coated with a nitrogen-doped Li_3PO_4 solid electrolyte (LiPON) of 110 to 180 nm in thickness, and finally with about 35 nm of a phosphorus-doped amorphous Si anode layer. A FEI Nova Nanolab 600 dual beam FIB/SEM (FEI, Hillsboro, OR, USA) [5] was used to expose the inner Ti/Pt/Ti cathode current collector and electrically isolate the anode from the cathode. Electron beam induced deposition was used to connect the electrodes to the Pt contact pads.

(S)TEM imaging, selected-area electron diffraction (SAED), and energy-dispersive X-ray (EDXS) and electron energy-loss spectroscopy (EELS) of functionalized SNWs and related devices were performed at a 300 kV accelerating voltage using a Schottky field-emission FEI Titan 80-300 analytical (S)TEM (FEI, Hillsboro, OR, USA) equipped with S-TWIN objective lenses. For high spatial resolution nanoanalyses in the STEM mode, the instrument was supplied with a Fischione 3000 model HAADF detector, BF- and ADF-STEM detectors, a 30 mm^2 EDAX Si/Li EDX detector with a 0.13 srad acceptance angle and a Gatan Enfina EEL spectrometer. To ensure optimal counting rates, the specimens were tilted 15 degrees towards the EDX detector.

3. Results and discussion

3.1. Uniform VLS-grown single-crystalline Si NWs

Device applications require reliable approaches for fabricating SNWs with controlled shapes and orientation. Single-crystalline <111> Si NWs were prepared via a two-stage VLS growth procedure for producing uniform NW arrays with a predominantly vertical orientation (Fig. 1a). Narrow diameter distributions (130 nm to 170 nm) of Si NWs were provided by the use of monodispersed Au nanoparticles (Fig. 1b). Typical cross-sections of NWs are hexagonal in shape with {112} facets as shown in right bottom inset of Fig. 1b. A SAED pattern in the [111] zone axis displays {220} point reflections indicating a single-crystalline structure of the diamond cubic type ($Fd\bar{3}m$ space group, left upper inset). HRTEM (left bottom inset, Fig. 1c) displays a defect-free area with two-dimensional 0.20-0.21 nm {220} lattice fringes near the NW's edge. Z-contrast STEM (Fig. 1c) shows a side view of a NW and an enlarged area with 0.32 nm (111) Si lattice spacing and a 4.3 nm-thick oxide layer confirmed by EDXS (right inset, Fig. 1e). A 3D plot of low-loss EEL spectra (Fig. 1d) was obtained from a line scan across an isolated NW. The spectra at the ends near 0 nm and 190 nm are aloof in vacuum, those at 25 nm and at 130 nm are just grazing the NW surface, and those in between

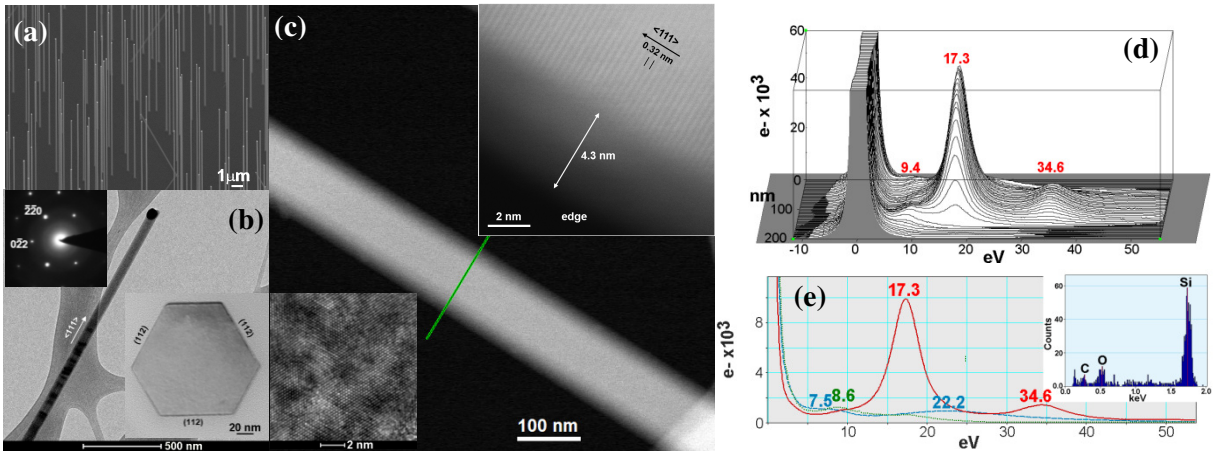

Figure 1. VLS-grown single-crystalline <111> Si NWs: (a) FESEM of a vertically aligned NW array. (b) BF-TEM, SAED (upper inset), and NW's cross-section (bottom inset) prepared by cutting, polishing and ion beam etching of NWs embedded into an epoxy resin. (c) HAADF STEM, 0.32 nm silicon (111) lattice fringes near the edge of the NW with no visible defects (upper inset), HRTEM, NW's cross-section (bottom inset). (d) 3D plot of STEM-EELS line profiling along the green line in (c). (e) Low-loss EEL spectra extracted from (d). X-ray spectrum (right inset in graph e) acquired at the oxide layer showing the Si-K peak at 1.74 keV and the O-K peak at 0.52 keV.

are penetrating the NW's bulk. The low-loss spectra are dominated by bulk plasmons at integer multiples of 17.3 eV (the first plasmon) and of 34.6 eV that correspond to the second plasmon (red line, Fig. 1e). As the beam reaches and passes the edge of the NW, the bulk plasmons disappear very rapidly and are replaced with surface plasmons between 8 eV to 10 eV energy losses (green dot line, Fig.1e). The peak at 7.5 eV is assigned to a Si/SiO_x interface plasmon (blue dashed line, Fig. 1e), which in the aloof mode also may be due in part to retardation effects [6]. The wide peak at about 22.2 eV (blue dashed line) corresponds to a bulk plasmon in SiO_x itself. These results illustrate possibilities for monitoring NW structures, including intentionally induced or native surface oxide layers that can be used for further functionalization or fabrication of semiconductor-oxide interfaces.

3.2. All-solid-state SNW core – multishell rechargeable Li-ion batteries

SNWs are highly attractive as building blocks in novel 3D multifunctional architectures for LiBs that maximize areal energy density. SNWs can be grown directly on the metallic current collector providing improvements in rate capabilities in metal oxide cathodes due to efficient 1D electron transport, reduced defects, and facile strain relaxation. With a focus on a miniature NW-LiB, we employ single-crystalline Si NWs as a scaffold for a complete (S)TEM–transparent all-solid-state nanobattery designed as a testing tool to correlate electrochemical performance with its hetero-structure arrangement and capture material transformations under cycling at the nanoscale *in situ* or *ex situ* [4]. STEM enables visualization of the internal microstructure of deposited active layers due to significant contrast variations even in 1.0 μm to 1.5 μm–thick areas, including textured $LiCoO_2$ crystallites of 160 nm to 200 nm in length and 30 nm to 60 nm in width that are tilted by 70 to 77° degrees towards the core and buried electrode–electrolyte interfaces as well (Fig. 2a). The texture of thermally grown hexagonal $LiCoO_2$ crystals ($R\bar{3}m$ space group) as found by HRTEM appeared with preferential orientations of Li-containing layers towards the core which is favorable for direct Li ion transport from the cathode to the current collector. Using high-tilt angle (±70°) HAADF STEM tomo-

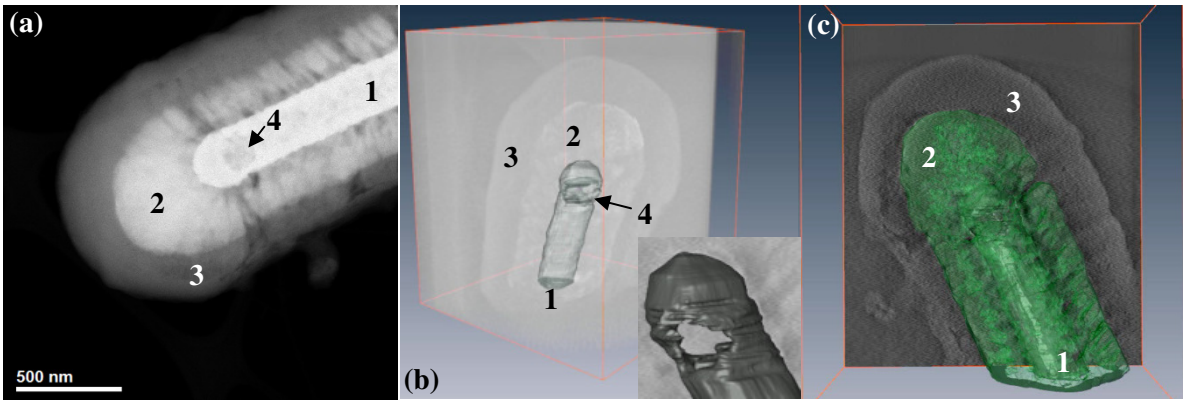

Figure 2. A NW-LiB: (a) HAADF-STEM tomography, a single frame extracted from a ±70 degree tilt-series. (b) The reconstructed 3D view of a NW-LiB's tip showing lateral distribution of $LiCoO_2$ crystallites around the segmented metallized NW core and a void (4) near its tip (inset). (c) 3D overlay of the segmented $LiCoO_2$ shell and the NW core. 1 - Si NW with a Ti/Pt/Ti metal collector layer, 2 - $LiCoO_2$ cathode layer, 3 - LiPON electrolyte layer covered with a n-Si amorphous anode layer.

graphy followed by a 3D reconstruction of the faceted metallized core with the simultaneous iterative reconstruction technique (SIRT), we revealed a void near the NW tip (bottom inset, Fig. 2b) that likely formed during annealing due to the reaction with the Pt-Ti metal collector (a Kirkendall effect), which was barely visible in 2D images. Furthermore, a 3D overlay of the segmented $LiCoO_2$ shell allows visualizing the complex morphology of the $LiCoO_2$ – LiPON interface (shown in green in Fig. 2c), where major electrochemical processes occur during cycling.

4. Summary

Analytical (S)TEM techniques enable critical insights into the 3D morphology, crystalline and electronic structures and chemical compositions of functionalized SNWs as prospective building blocks that are suitable for both a large scale-up synthesis and fabrication using existing technologies for a variety of emerging applications. Furthermore, new designs of SNW-based lab-on-a-chip devices may allow for direct correlation between electrical transport and (electro)chemical properties tailored for specific performance with the unique axial and radial heterostructure morphology and atomic arrangement on the same nanoscale structure being analyzed in various (S)TEM modes.

Acknowledgements

The support by NIST under Grant MML12-1053-N00 is gratefully acknowledged (VPO).

References

[1] Williams E H, Schreifels J A, Rao M V, Davydov A, Oleshko V P, Lin N, Steffens K, Krylyuk S, Bertness K, Manocchi A, Koshka Y 2013 *J Mater Res* **28** 68
[2] Aluri G S, Motayed A, Davydov A V, Oleshko V P, Bertness K A, Sanford N A, Rao, M V 2012 *Nanotechnol* **23** 175501
[3] Bajpai R, Motayed A, Davydov A V, Oleshko V P, Aluri G S, Bertness K A, Rao M V, Zaghloul M E 2012 *Sensors Actuators B: Chem* **171-172** 499
[4] Ruzmetov D, Oleshko V P, Haney P M, Lezec H, Karki K, Baloch K H, Agrawal A K, Davydov A V, Krylyuk S, Liu Y, Huang J Y, Tanase M, Cumings J, Talin A A 2012 *Nano Letters* **12** 505
[5] Commercial equipment and materials are identified in this document to adequately describe experimental procedures. This does not imply endorsement by NIST.
[6] Moreau P, Brun N, Walsh C A, Colliex C, Howie A 1997 *Phys Rev B* **56** 6774